

Formation mechanism of MgB₂ in 2LiBH₄ + MgH₂ system for reversible hydrogen storage

KOU Hua-qin, XIAO Xue-zhang, CHEN Li-xin, LI Shou-quan, WANG Qi-dong

Department of Materials Science and Engineering, Zhejiang University, Hangzhou 310027, China

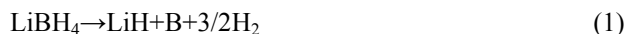
Received 16 May 2010; accepted 29 November 2010

Abstract: The formation conditions of MgB₂ in 2LiBH₄ + MgH₂ system during dehydrogenation were investigated and its mechanism was discussed. The results show that direct decomposition of LiBH₄ is suppressed under relative higher initial dehydrogenation pressure of 4.0×10⁵ Pa, wherein LiBH₄ reacts with Mg to yield MgB₂, and 9.16% (mass fraction) hydrogen is released within 9.6 h at 450 °C. However, under relatively lower initial dehydrogenation pressure of 1.0×10² Pa, LiBH₄ decomposes independently instead of reacting with Mg, resulting in no formation of MgB₂, and 7.91% hydrogen is desorbed within 5.2 h at 450 °C. It is found that the dehydrogenation of 2LiBH₄ + MgH₂ system proceeds more completely and more hydrogen desorption amount can be obtained within a definite time by forming MgB₂. Furthermore, it is proposed that the formation process of MgB₂ includes incubation period and nucleus growth process. Experimental results show that the formation process of MgB₂, especially the incubation period, is promoted by increasing initial dehydrogenation pressure at constant temperature, and the incubation period is also influenced greatly by dehydrogenation temperature.

Key words: complex hydride; LiBH₄; MgB₂; hydrogen storage; formation mechanism

1 Introduction

Hydrogen is an ideal secondary energy carrier for application because of its highly energy content and environmental harmony. However, efficient hydrogen storage and transportation is a key technical challenge in promoting its further applications. LiBH₄, which owns high gravimetric and volumetric hydrogen densities (18.5% in mass fraction and 121 kg/m³), has been regarded as one of the most promising hydrogen storage materials[1]. The hydrogen desorption reaction at elevated temperature (>400 °C) proceeds as follows[2]:

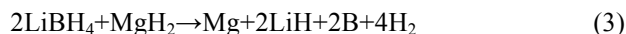


Upon the overall dehydriding reaction, 13.5% of hydrogen can be released from LiBH₄. Unfortunately, it is experimentally shown that LiBH₄ is thermodynamically stable for practical use, and it is required for extremely rigorous reaction conditions to reverse[3–4]. VAJO et al[5–6] developed a hydrogen storage system composed of LiBH₄ and MgH₂, in which LiBH₄ was effectively destabilized and reaction

reversibility was improved. The reversible dehydrogenation/rehydrogenation reaction is expressed as follows:



Interestingly, previous experiments show that a hydrogen atmosphere is necessary for dehydrogenation according to reaction (2). If under dynamic vacuum, however, MgB₂ is not formed, and dehydrogenation follows another reaction path expressed as[7]



Meanwhile, calorimetric measurements by NAKAGAWA et al[8] showed the formation of MgB₂ unless under H₂ atmosphere rather than inert gas. PRICE et al[9–11] found that the dehydrogenation pathway was hardly affected by the stoichiometry ratio of LiBH₄ to MgH₂ and Li-Mg alloy was formed under dynamic vacuum after dehydrogenation at high temperature. PINKERTON et al[7] reported a thermodynamically and kinetically boundaries of the H₂ pressure–temperature for formation of MgB₂ in TiCl₃-catalyzed 2LiBH₄+MgH₂ system. A wide sloping plateau was observed by

BÖSENBERG et al[12] during dehydrogenation of neat $2\text{LiBH}_4+\text{MgH}_2$ system. However, there is still no further investigation on appearance reason of the plateau. Although the impact of hydrogen atmosphere on the appearance of MgB_2 in the product has been studied extensively, little investigation on full understand of the formation of MgB_2 has been done as yet.

Because MgB_2 plays an important role in reversible hydrogen storage, it is significant to reveal the detailed connection between comprehensive reaction conditions and formation of MgB_2 . Therefore, in the present work, we investigated the intrinsic formation mechanism of MgB_2 during the dehydrogenation of $2\text{LiBH}_4+\text{MgH}_2$ system.

2 Experimental

LiBH_4 (95% in mass fraction) and MgH_2 (98% in mass fraction) were purchased from Alfa Aesar Corp. All materials were used as-received in powder form. The sample of $2\text{LiBH}_4 + \text{MgH}_2$ system was mechanically milled under 1 MPa hydrogen pressure in a Planetary mill at 400 r/min for 2 h. The milling vessel and balls were made of stainless steel. The ball to powder mass ratio was in around 40:1. All sample operations were performed in a glovebox under continuous purified argon atmosphere. Hydrogen desorption behaviors of the samples were monitored with a Sievert's type apparatus. Dehydrodring performance started from a finite initial hydrogen pressure with heating to aimed temperature at a constant ramping rate of $5\text{ }^\circ\text{C}/\text{min}$. Each time, 150–250 mg sample was put into a closed large reaction sample volume (820 mL), which resulted in $(0.2\text{--}0.3)\times 10^5$ Pa pressure change after dehydrogenation. The identification of the samples was carried out by X-ray diffractometry (XRD, X'Pert-PRO, Cu K_α radiation). To prevent H_2O and O_2 contamination during the measurements, a special sample holder was used.

3 Results and discussion

3.1 Investigation on dehydrogenation process of $2\text{LiBH}_4+\text{MgH}_2$ system

The dehydrodring behaviors of $2\text{LiBH}_4 + \text{MgH}_2$ system were measured firstly by heating to $450\text{ }^\circ\text{C}$ and under initial dehydrogenation pressure of 1.0×10^2 Pa and 4.0×10^5 Pa, respectively, as shown in Fig.1. Because the pressure increase during the dehydrogenation is small, the initial dehydrogenation pressure almost presents the reaction pressure circumstance. It can be seen that the dehydrodring curve under 1.0×10^2 Pa initial hydrogen gas back-pressure exhibits a two-step feature, whereas roughly three-step feature under 4.0×10^5 Pa initial dehydrogenation pressure. For both samples, their first

dehydrogenation steps are similar, after which about 2.5% hydrogen is released. Evident difference appears after the first dehydrogenation step. Under 1.0×10^2 Pa initial dehydrogenation pressure, hydrogen is released acutely as temperature increases, reaching 7.91% within 5.2 h at $450\text{ }^\circ\text{C}$. In comparison, the dehydrodring curve under 4.0×10^5 Pa initial dehydrogenation pressure exhibits a sloping plateau with slow hydrogen desorption. However, about 6 h later, hydrogen then evolves rapidly, and hydrogen desorption capacity of 9.16% is finally obtained within 9.6 h.

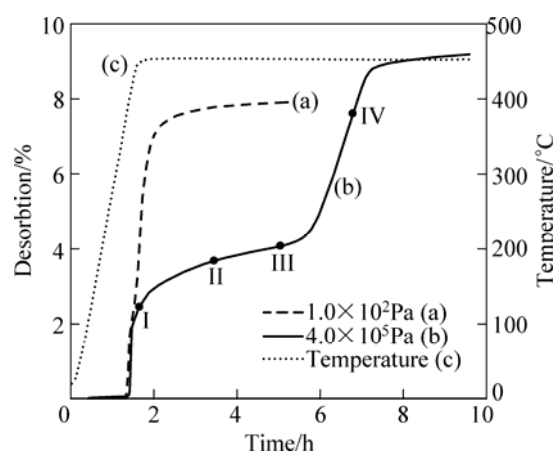


Fig.1 Dehydrodring curves of $2\text{LiBH}_4+\text{MgH}_2$ systems performed under initial dehydrogenation pressure of 1.0×10^2 Pa (a) and 4.0×10^5 Pa (b) and temperature profile (c) at ramping rate of $5\text{ }^\circ\text{C}/\text{min}$

Figure 2 shows the XRD patterns of the dehydrodring samples performed under 1.0×10^2 Pa and 4.0×10^5 Pa initial dehydrogenation pressure, respectively. When an initial dehydrodring pressure of 4.0×10^5 Pa is applied, MgB_2 , Mg and LiH are produced (Fig.2(b)). On the other hand, when an initial hydrogen pressure of 1.0×10^2 Pa is applied, three phases of Mg, B and LiH are

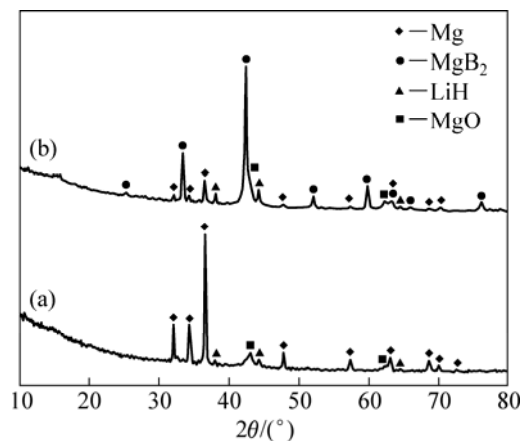


Fig.2 XRD patterns of dehydrodring $2\text{LiBH}_4+\text{MgH}_2$ systems performed under initial dehydrodring pressures of 1.0×10^2 Pa (a) and 4.0×10^5 Pa (b)

produced (Fig.2(a)). Unfortunately, no diffraction peak of boron can be observed, suggesting that boron is amorphous, which agreed with other references[2–3]. These results confirm the impact of initial dehydrogenation pressure on dehydrating products of $\text{LiBH}_4\text{-MgH}_2$ system that the formation of MgB_2 needs hydrogen overpressure of a fraction of MPa, and relatively lower initial H_2 gas back-pressure leads to Mg and B produced instead of MgB_2 . A little MgO phase may be caused by oxidation during loading. The broad peak around $2\theta=15^\circ$ corresponds to the thin film of sample holder.

To understand the formation process of MgB_2 and the effectiveness of the plateau in the dehydrating curve under 4.0×10^5 Pa initial dehydrogenation pressure, we performed XRD phase analysis at the different dehydrating stages (I, II, III and IV points in Fig.1(b)) in the dehydrogenation process, as shown in Fig.3. Figure 3(a) shows the XRD pattern of $2\text{LiBH}_4 + \text{MgH}_2$ mixture prepared by mechanical milling. After dehydrogenation proceeding for 1.7 h, the XRD pattern in Fig.3(b) corresponds to LiBH_4 and Mg metal, indicating that MgH_2 has decomposed into Mg and H_2 relative to the first dehydrogenation step, described as reaction (4). For XRD pattern in Fig.3(c) corresponding to dehydrating for 3.5 h, there is a little LiH besides LiBH_4 and Mg, but no MgB_2 appears, which can be seen from the illustrated pattern. This indicates that a small amount of LiBH_4 has decomposed. Then, nearly no changes display in Fig.3(d) after dehydrating for 5 h, which is in accordance with the appearance of plateau in Fig.1(b). However, strong peaks of MgB_2 arise when the reaction duration extends to 6.8 h, as shown in Fig.3(e). Meanwhile, some LiBH_4 and Mg are detected still. After the overall dehydrogenation completed about 9.6 h later, massive MgB_2 has formed and a small quantity of Mg is obtained, and no LiBH_4 can be observed simultaneously (Fig.2(b)). This suggests that MgB_2 is formed from the reaction of LiBH_4 and Mg, which can be described as reaction (5). Combined with the dehydrating curve of Fig.1(b), the dehydrating process of $2\text{LiBH}_4 + \text{MgH}_2$ system under 4.0×10^5 Pa initial dehydrogenation pressure can be described as follows: along with temperature increasing to 450°C , MgH_2 is firstly decomposed, forming Mg and releasing H_2 ; when temperature holding at 450°C , a small amount of LiBH_4 is slowly decomposed; over 6 h extending, MgB_2 is uninterruptedly produced accompanying with a large amount of H_2 evolved. Thus, the dehydrogenation process of $2\text{LiBH}_4 + \text{MgH}_2$ at 450°C under 4.0×10^5 Pa initial dehydrogenation pressure can be summarized as three steps: 1) decomposition of MgH_2 to form Mg and H_2 ; 2) decomposition of a small amount of LiBH_4 ; 3) fast dehydrogenation of LiBH_4 to react with Mg and form MgB_2 . Obviously, steps 2) and 3) present two

dehydrogenation pathways of $\text{LiBH}_4\text{-MgH}_2$ system under relatively higher initial dehydrogenation pressure and relatively lower initial dehydrogenation pressure, respectively.

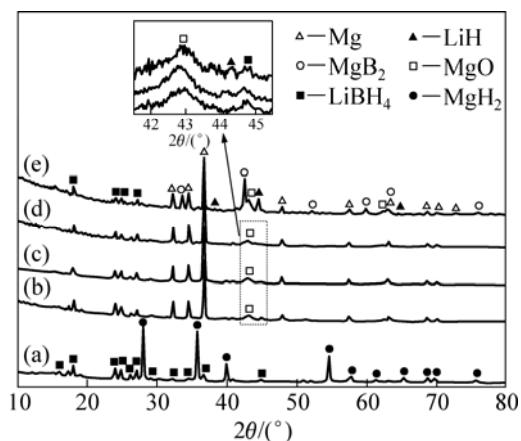
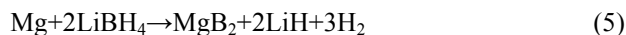


Fig.3 XRD patterns of $2\text{LiBH}_4 + \text{MgH}_2$ systems at different dehydrating stages performed under 4.0×10^5 Pa initial dehydrogenation pressure before dehydrogenation (a) and after dehydrating for 1.7 h (b), 3.5 h (c), 5 h (d) and 6.8 h (e) (Peak identifications of LiBH_4 are originated from Ref.[3].)

It can be found that dehydrogenation pathway under higher initial pressure (recorded as DP(1)) is the sequence of reaction (4) and reaction (5). However, dehydrogenation pathway under lower initial pressure (recorded as DP(2)) is nothing but the result of physical stacking of reaction (4) and reaction (1). The key difference between DP(1) and DP(2) originates from the second dehydrogenation reaction. Under relatively higher initial dehydrogenation pressure, direct decomposition of LiBH_4 is suppressed and LiBH_4 can react with Mg to yield MgB_2 . Conversely, LiBH_4 decomposes independently under relatively lower initial dehydrogenation pressure. So, the dehydrogenation pathway is greatly dependence of reaction hydrogen pressure.

3.2 Investigation on influence of initial dehydrogenation pressure

Figure 4 shows dehydrating behaviors of $2\text{LiBH}_4 + \text{MgH}_2$ system applied to different initial hydrogen pressures from room temperature to 450°C . The dehydrating curves under 1.0×10^5 Pa and 2.0×10^5 Pa initial hydrogen pressure demonstrate a two-step dehydrogenation. For both of them, the first step is similar, with desorbed hydrogen of about 2.5%. However, the second hydrogen desorption step under 2.0×10^5 Pa initial hydrogen pressure is slower than that under

1.0×10^5 Pa. After holding at 450°C for 13 h, desorption of 8.05% and 8.12% hydrogen are released under 1.0×10^5 Pa and 2.0×10^5 Pa initial hydrogen pressure, respectively. Three-step dehydrogenation is obviously observed under 3.0×10^5 Pa and 4.0×10^5 Pa together with 4.8×10^5 Pa initial hydrogen pressure, in all which dehydrating plateau and fast releasing of hydrogen after the plateau can be identified. Furthermore, it can be found that the hydrogen desorption rate of the second step corresponding to decomposition of LiBH_4 and dehydrating plateau become slower and shorter with increasing initial pressure. These plateaus consume approximately are 7.5, 4 and 3 h for initial hydrogen pressure of 3.0×10^5 , 4.0×10^5 , 4.8×10^5 Pa, respectively. Simultaneously, the hydrogen desorption rate in the third step increases gradually with increasing initial hydrogen pressure. As a result, 9.1% and 9.0% hydrogen have been released within 9 h under 4.0×10^5 Pa and 4.8×10^5 Pa initial hydrogen pressure, while 7.9% hydrogen is released within even 13 h under 3.0×10^5 Pa initial hydrogen pressure. It can be concluded that more complete dehydrogenation of $2\text{LiBH}_4 + \text{MgH}_2$ occurs and more hydrogen desorption amount can be obtained within a definite time with increasing initial dehydrogenation pressure.

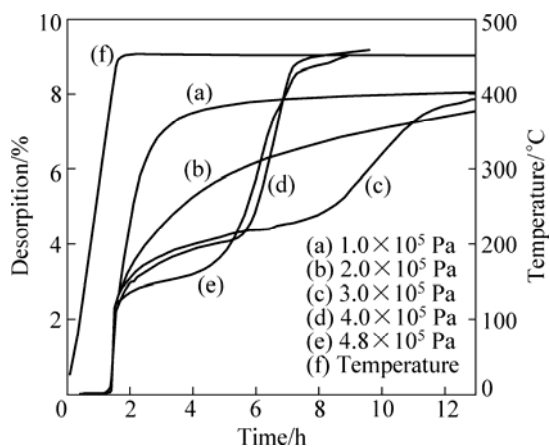


Fig.4 Dehydrating curves of $2\text{LiBH}_4 + \text{MgH}_2$ systems performed under different initial dehydrogenation pressures and temperature profile at temperature ramping rate of $5^\circ\text{C}/\text{min}$

The XRD patterns of the dehydrogenated $2\text{LiBH}_4 + \text{MgH}_2$ samples applied to different initial hydrogen pressures are shown in Fig.5. All dehydrating products of different initial hydrogen pressures consist of Mg, MgB_2 and LiH. Nevertheless, the peak intensity of Mg appears much weaker along with increasing hydrogen pressure, while the peak intensity of MgB_2 appears much stronger. Compared the products of reaction (2) with reaction (3), it is found that LiH exists in both reactions. Simultaneously, it is noteworthy that boron produced in reaction (3) cannot be characterized

by XRD[2–3]. Therefore, the dehydrated product, Mg or MgB_2 , is the signal of each dehydrogenation pathway. MgB_2 represents DP(1), while the presence of Mg metal in the products represents DP(2). Due to the LiBH_4 to Mg molar ratio of 2:1, the relative content of MgB_2 to Mg in the products implies that the relative proportion of LiBH_4 that reacts with Mg or decomposes independently. In other words, the relative diffraction intensity of MgB_2 to Mg metal in the XRD patterns implies the occurrence rate of DP(1) or DP(2) in the overall dehydrogenation. If only MgB_2 phase exists in the products, it means that the whole dehydrogenation reaction proceeds as DP(1). The dehydrogenation reaction entirely follows DP(2), in contrast, only when Mg metal phase exists in the products. According to Fig. 5, we can conclude that both DP(1) and DP(2) appear in the whole dehydrogenation reaction under various initial hydrogen pressures. However, with increasing the initial dehydrogenation pressure, dehydrogenation prefers to follow DP(1).

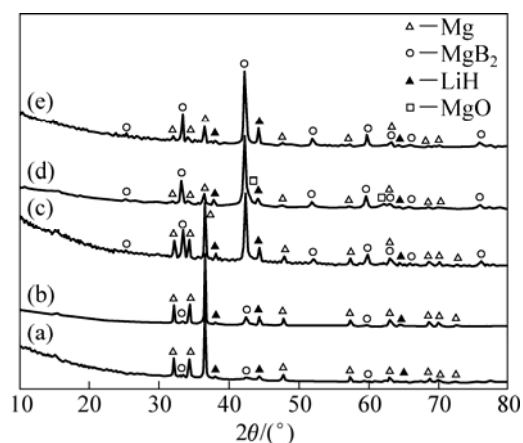


Fig.5 XRD patterns of dehydrogenated $2\text{LiBH}_4 + \text{MgH}_2$ systems performed under initial dehydrogenation pressures of 1.0×10^5 Pa (a), 2.0×10^5 Pa (b), 3.0×10^5 Pa (c), 4.0×10^5 Pa (d) and 4.8×10^5 Pa (e)

3.3 Investigation on influence of dehydrogenation temperature

Figure 6 shows the dehydrating curve of $2\text{LiBH}_4 + \text{MgH}_2$ system from room temperature to 500°C under 4.0×10^5 Pa initial hydrogen pressure. It can be seen that no dehydrating plateau appears after the first desorption step, and hydrogen is rapidly released along with temperature rising. Finally, a dehydrating capacity of 8.49% is obtained within 5 h. The XRD pattern of the dehydrogenated product is shown in Fig.7(a). Unfortunately, a large amount of unexpected Mg metal remained, besides some MgB_2 formed. From the relative diffraction intensity of MgB_2 to Mg metal in the XRD pattern, we infer that the main proportion of LiBH_4 is decomposed independently, and a small amount of LiBH_4 retains for reacting with Mg to produce MgB_2 . It

suggests that, although the dehydrogenating rate is improved, the temperature of 500 °C is too high to suppressing direct decomposition of LiBH_4 under 4.0×10^5 Pa initial hydrogen pressure. The presence of MgH_2 in the products probably originated from rehydrogenation of Mg metal during air cooling from 500 °C to room temperature under the hydrogen pressure of 4.0×10^5 Pa.

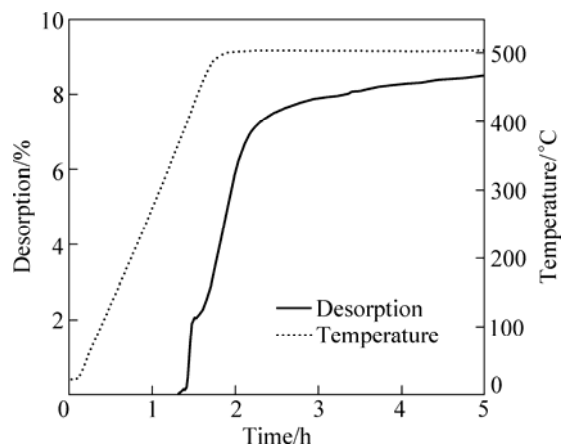


Fig.6 Dehydrodring curve of $2\text{LiBH}_4 + \text{MgH}_2$ system from room temperature to 500 °C under 4.0×10^5 Pa initial hydrogen pressure and temperature ramping rate of 5 °C/min

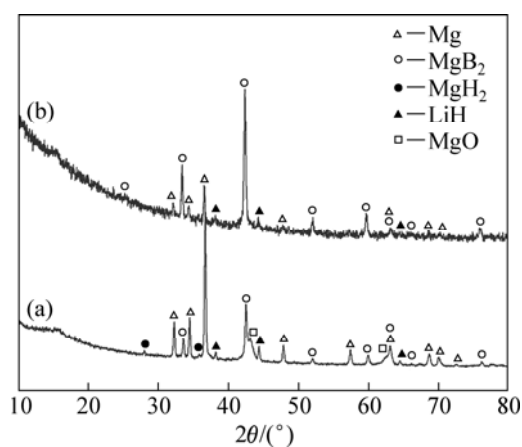


Fig.7 XRD patterns of dehydrodringated $2\text{LiBH}_4 + \text{MgH}_2$ systems performed under different conditions: (a) RT -500 °C for 5 h; (b) RT -400 °C for 15 h, then increased to 450 °C for 13 h

Figure 8 shows the dehydrodring curve of $2\text{LiBH}_4 + \text{MgH}_2$ system from room temperature to 400 °C then increased to 450 °C under 4.0×10^5 Pa initial hydrogen pressure. It is found that the dehydrodring plateau at 400 °C is quite flat, suggesting that the decomposition of LiBH_4 is suppressed significantly. At this time, the amount of hydrogen desorbed almost maintains at 2.8% and no trace of the formation of MgB_2 (massive hydrogen is released abruptly) appears until temperature increases to 450 °C, even though dehydrodring plateau extends to 15 h at 400 °C. The phase composition after

dehydrodringation is given in Fig.7(b). The relative diffraction intensity of MgB_2 in the final product, which is similar to that in Fig.2(b), is in agreement with the dehydrodring behavior shown in Fig.8. This indicates that the temperature of 400 °C is not high enough to facilitate the formation of MgB_2 in $2\text{LiBH}_4 + \text{MgH}_2$ system, though the direct decomposition of LiBH_4 is suppressed effectively. As a result, it can be concluded that the temperature of 450 °C is proper for the formation of MgB_2 in the $2\text{LiBH}_4 + \text{MgH}_2$ system under 4.0×10^5 Pa initial dehydrodringation pressure.

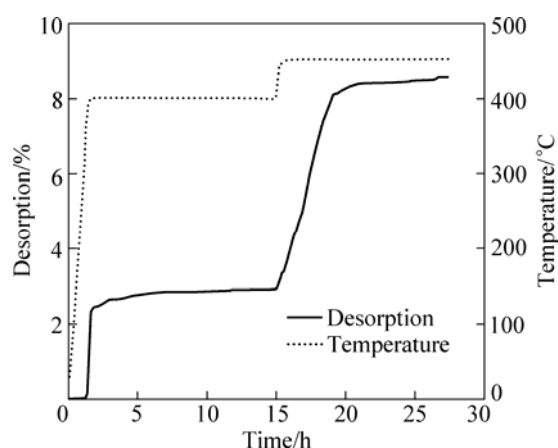


Fig.8 Dehydrodring curve of $2\text{LiBH}_4 + \text{MgH}_2$ system from room temperature to 400 °C and then increased to 450 °C under 4.0×10^5 Pa initial hydrogen pressure (at 400 °C for 15 h and at 450 °C for 13 h, temperature ramping rate of 5 °C/min)

On the basis of above results, it is found that the dehydrodringation of $2\text{LiBH}_4 + \text{MgH}_2$ system proceeds more completely and more hydrogen desorption capacity can be obtained within a definite time by forming MgB_2 than separated decomposition of LiBH_4 and MgH_2 . Actually, the formation process of MgB_2 obeys the general features of nucleation, in particular, the effect of supercool or superheat and component concentration on the potency of nucleation: 1) the increase of the supercool degree or superheat degree can enhance the nucleation; 2) the nucleation potency improves with the component concentration of the reactants close to stoichiometric ratio of the product[13–14].

In general, the nucleation rate increases dramatically along with superheat rising, resulting in that the incubation is shortened significantly[15]. According to the above experiment results, it is found that the formation of MgB_2 indeed requires an incubation period, exhibiting as a plateau in the dehydrodring curve, which is greatly affected by reaction temperature. It shows that elevated temperature promotes the incubation of MgB_2 , and the ability of incubation is deteriorated at the decreased temperature. Furthermore, it shows that the component concentration of LiBH_4 to Mg is maintained

more closer to 2:1 during the dehydrogenating plateau, the incubation process for MgB_2 is more favorable, and vice versa. Under the lower hydrogen gas back-pressure, LiBH_4 is decomposed quickly, resulting in little LiBH_4 remained for the incubation of MgB_2 . Due to the relatively higher hydrogen gas back-pressure inhibiting the decomposition of LiBH_4 , there is sufficient LiBH_4 for incubation of MgB_2 . As a result, the component concentration of LiBH_4 to Mg is maintained more closer to 2:1 during the dehydrogenating plateau under relatively higher hydrogen gas back-pressure than the lower hydrogen gas back-pressure. So, it can be seen from Fig.4 that the incubation period is shortened by increasing hydrogen gas back-pressure. Consequently, it is inferred that the incubation period of 1.0×10^5 Pa or 2.0×10^5 Pa initial dehydrogenation pressure is much longer than that of 3.0×10^5 Pa. The reason that the incubation plateau was not observed clearly was that the majority of LiBH_4 decomposed independently and only a small amount of LiBH_4 reacted with Mg to produce MgB_2 , which was good consistent with the XRD reflection result. On the basis of above analysis, it is suggested that the plateau of the dehydrogenating curve relates to the incubation period for nucleation of MgB_2 , after which it should be the rapid growth of nucleus accompanying with a large amount of H_2 released.

At the same time, the results show that none of the involved experiments in this work entirely followed DP(1) to produce only MgB_2 rather than Mg . Because MgB_2 plays a key role in the reversibility of LiBH_4 - MgH_2 system, the full formation of MgB_2 is necessary during the dehydrogenation of $2\text{LiBH}_4 + \text{MgH}_2$ system. In fact, there are two ways to make the dehydrogenation of $2\text{LiBH}_4 + \text{MgH}_2$ system just only follow DP(1): first one is to violently suppress the direct decomposition of LiBH_4 . Generally, increasing initial dehydrogenation pressure can improve the ability in suppressing the decomposition of LiBH_4 at constant temperature. However, excess high pressure will inevitably lead to the decomposition of MgH_2 in harsh condition. Thus, the hydrogen pressure applied in the decomposition of LiBH_4 should be as low as possible. In this case, it shows that an applied hydrogen pressure of at least 4.0×10^5 Pa is potentially appropriate to obtain comprehensive ability in yielding MgB_2 at 450°C in $2\text{LiBH}_4 + \text{MgH}_2$ system. Nevertheless, a small sealed reaction volume may be used for dehydrogenation of $2\text{LiBH}_4 + \text{MgH}_2$ system under relative lower initial dehydrogenation pressure or vacuum, through which not only MgH_2 decomposes readily but also there is sufficient hydrogen pressure to suppress the direct decomposition of LiBH_4 after the decomposition of MgH_2 . The other way for the full formation of MgB_2 is to make the incubation period very short so that the

reaction of LiBH_4 with Mg occurs quickly before the separated decomposition of LiBH_4 . Adding nucleating agent or catalysts may be a useful method for that purpose. So, it seems that using a proper small sealed reaction volume with nucleating agent or catalyst is a potentially effective strategy for improving the comprehensive properties of $2\text{LiBH}_4 + \text{MgH}_2$ system, which is being investigated currently.

4 Conclusions

1) The dehydrogenation pathway of $2\text{LiBH}_4 + \text{MgH}_2$ system was investigated carefully. It is found that the dehydrogenation pathway is determined by initial dehydrogenation pressure, which suppresses the direct decomposition of LiBH_4 or not.

2) Under relatively higher initial dehydrogenation pressure, LiBH_4 reacts with Mg to produce MgB_2 . However, under relatively lower initial dehydrogenation pressure, LiBH_4 is decomposed independently, resulting in no formation of MgB_2 .

3) The dehydrogenation of $2\text{LiBH}_4 + \text{MgH}_2$ system proceeds more completely and more hydrogen desorption amount can be obtained within a definite time by forming MgB_2 .

4) The formation process of MgB_2 consisting of incubation period and nucleus growth process is proposed. The results show that the formation process of MgB_2 is enhanced by increasing initial dehydrogenation pressure at constant temperature. Additionally, elevated temperature could significantly reduce incubation period, while the ability to suppress the decomposition of LiBH_4 is deteriorated under a finite hydrogen gas back-pressure.

References

- [1] SCHLAPBACH L, ZÜTTEL A. Hydrogen-storage materials for mobile applications [J]. *Nature*, 2001, 414: 353–358.
- [2] ZÜTTEL A, WENGER P, RENTSCH S, SUNDAN P, MAURON P H, EMMENEGGER C H. LiBH_4 a new hydrogen storage material [J]. *Journal of Power Sources*, 2003, 118(1–2): 1–7.
- [3] ORIMO S, NAKAMORI Y, KITAHARA G, MIWA K, OHBA N, TOWATA S, ZÜTTEL A. Dehydrogenating and rehydrogenating reactions of LiBH_4 [J]. *Journal of Alloys and Compounds*, 2005, 404–406: 427–430.
- [4] ZÜTTEL A, RENTSCH S, FISCHER P, WENGER P, SUNDAN P, MAURON P H, EMMENEGGER C H. Hydrogen storage properties of LiBH_4 [J]. *Journal of Alloys and Compounds*, 2003, 356–357: 515–520.
- [5] VAJO J J, SKEITH S L, MERTENS F. Reversible storage of hydrogen in destabilized LiBH_4 [J]. *The Journal of Physical Chemistry B*, 2005, 109(9): 3719–3722.
- [6] VAJO J J, OLSON G L. Hydrogen storage in destabilized chemical systems [J]. *Scripta Materialia*, 2007, 56(10): 829–834.
- [7] PINKERTON F, MEYER M S, MEISNER G P, BALOGH M P, VAJO J J. Phase boundaries and reversibility of $\text{LiBH}_4/\text{MgH}_2$ hydrogen storage material [J]. *The Journal of Physical Chemistry C*,

- 2007, 111(35): 12881–12885.
- [8] NAKAGAWA T, ICHIKAWA T, HANADA N, KOJIMA Y, FUJII H. Thermal analysis on the Li-Mg-B-H systems [J]. *Journal of Alloys and Compounds*, 2007, 446–447: 306–309.
- [9] PRICE T E C, GRANT D M, TELEPANI I, YU X B, WALKER G S. The decomposition pathways for $\text{LiBD}_4\text{-MgD}_2$ multicomponent systems investigated by in situ neutron diffraction [J]. *Journal of Alloys and Compounds*, 2009, 472(1–2): 559–564.
- [10] WALKER G S, GRANT D M, PRICE T E C, YU X B, LEGRAND V. High capacity multicomponent hydrogen storage materials: Investigation of the effect of stoichiometry and decomposition conditions on the cycling behaviour of $\text{LiBH}_4\text{-MgH}_2$ [J]. *Journal of Power Sources*, 2009, 194(2): 1128–1134.
- [11] YU X B, GRANT D M, WALKER G S. A new dehydrogenation mechanism for reversible multicomponent borohydride systems—The role of Li-Mg alloys [J]. *Chemical Communications*, 2006(36): 3906–3908.
- [12] BÖSENBERG U, DOPPIU S, MOSEGAARD L, BARKHORDARIAN G, EIGEN N, BORGSCHULTE A, JENSEN T R, CERENIUS Y C, GUTEISCH O, KLASSEN T, DORNHEIM M, BORMANN, R. Hydrogen sorption properties of $\text{MgH}_2\text{-LiBH}_4$ composites [J]. *Acta Materialia*, 2007, 55(11): 3951–3958.
- [13] TEN WOLDE P R, FRENKEL D. Enhancement of protein crystal nucleation by critical density fluctuations [J]. *Science*, 1997, 277(5334): 1975–1978.
- [14] VEKILOV P G. Two-step mechanism for the nucleation of crystals from solution [J]. *Journal of Crystal Growth*, 2005, 275(1–2): 65–76.
- [15] THOMAS J J. A new approach to modeling the nucleation and growth kinetics of tricalcium silicate hydration [J]. *Journal of the American Ceramic Society*, 2007, 90(10): 3282–3288.

2LiBH₄+MgH₂ 体系放氢过程中 MgB₂ 的形成机理

寇化秦, 肖学章, 陈立新, 李寿权, 王启东

浙江大学 材料科学与工程学系, 杭州 310027

摘要: 对 $2\text{LiBH}_4\text{+MgH}_2$ 体系放氢过程中 MgB_2 的形成条件及机理进行研究。结果表明: 在较高的 $4.0\times 10^5\text{ Pa}$ 初始氢背压下放氢时, 会抑制 $2\text{LiBH}_4\text{+MgH}_2$ 体系中 LiBH_4 的自行分解, 进而使其与 MgH_2 分解放氢后生成的 Mg 发生反应生成 MgB_2 , 同时在 $450\text{ }^\circ\text{C}$ 、 9.6 h 内释放出 9.16% (质量分数)的氢气; 而在较低的 $1.0\times 10^2\text{ Pa}$ 初始氢背压下放氢时, 体系中 LiBH_4 会先行发生自行分解, 从而不能与 Mg 发生反应生成 MgB_2 , 在 $450\text{ }^\circ\text{C}$ 、 5.2 h 内只能放出 7.91% 的氢气。 $2\text{LiBH}_4\text{+MgH}_2$ 体系放氢生成 MgB_2 可以使放氢反应进行得更彻底, 并释放出更多的氢气。 $2\text{LiBH}_4\text{+MgH}_2$ 放氢时 MgB_2 的形成过程是一个孕育-长大的过程, 随着氢背压的增高, 孕育期缩短; 而随着反应温度的降低, 孕育期延长。

关键词: 配位氢化物; LiBH_4 ; MgB_2 ; 储氢; 形成机理

(Edited by YANG Hua)